FERMILAB-PUB-82-112-E

Rockefeller University
Report No. RU 81/A-17
E-396

CHARGED MULTIPLICITIES of HIGH MASS DIFFRACTIVE $\pi^{\pm}$, $K^{\pm}$ and $p^{\pm}$ STATES

R.L. Cool, K. Goulianos, S.L. Segler[(a)],
H. Sticker and S.N. White
The Rockefeller University, New York, NY 10021

ABSTRACT

We report a measurement of charged multiplicity distributions of high mass diffractive $\pi^{\pm}$, $K^{\pm}$ and $p^{\pm}$ states produced in 100 and 200 GeV/c hadron-proton collisions, $h + p \rightarrow X + p$. The distributions are described well by a Gaussian function that depends only on the available mass $M = (M_x - M_h)$ (GeV), has a maximum at $n_o \cong 2M^{\frac{1}{2}}$ and a peak to width ratio $n_o/D \cong 2$.

(Submitted to Physical Review Letters)

We have measured the charged multiplicities of the diffractive states X produced in the reaction

$$h + p \rightarrow X + p \quad (h = \pi^{\pm}, K^{\pm}, p^{\pm}) \tag{1}$$

at incident beam momenta of 100 and 200 GeV/c in the kinematic range $0.025 < |t| < 0.095\ (\mathrm{GeV/c})^2$ and $1-x \cong (M_x^2 - M_h^2)/s < 0.1$, where t is the square of the four-momentum transfer, M_x is the hadron excitation mass, and x is the Feynman scaling variable. These measurements were performed in the course of experiment E-396 at Fermilab. Results from this experiment on the M_x^2 distribution and on the factorization properties of reaction (1), reported previously[1], shed light on the production dynamics of the high mass diffractive states, in particular on the role of the triple Pomeron coupling. The charged multiplicities provide insight into their decay mechanism. In this report, we present the data and describe their general characteristics. In another publication[2] we relate the diffractive multiplicities to hadronic multiplicities in general.

The experiment was performed in a tagged hadronic beam, the M6W beam line. The apparatus, which is described in detail in previous publications discussing the elastic scattering[3] and the diffraction dissociation[1] results, consisted of a gas H_2 target at atmospheric pressure and a detector that measured the polar angle, θ, and the kinetic energy, T, of protons recoiling from the interaction point. The missing mass was determined, to an accuracy of $\Delta M_x^2/M_x^2 = 3\%$, from θ, T and the incident momentum, p_o :

$$M_x^2 = M_h^2 + 2p_o \sqrt{2m_pT} \; (\cos\theta - \sqrt{T/2m_p}) \qquad (2)$$

The charged multiplicities were obtained from the pulse height recorded by two scintillation counters located downstream of the recoil detector. The two counters were cross-calibrated using elastic scattering events. Landau fluctuations were reduced by accepting the smaller of the two pulse heights. An example of a pulse height distribution for a particular M_x^2 bin is shown in Figure 2. One can see that low multiplicities are well resolved but some overlap occurs at high multiplicities. The pulse height spectra were fitted to Landau distributions, calculated for each multiplicity, using the maximum likelihood method. The curve in Figure 2 represents such a fit.

The raw multiplicities obtained in this manner were corrected for background tracks, for extra (accidental) beam particles and for the acceptance of the multiplicity counters. The background was estimated by using events with negative (unphysical) M_x^2 and was subtracted from the topological cross sections at the corresponding positive M_x^2. The subtractions were generally less than 10%. The fraction of events with an extra beam track was measured to be $\lesssim 10\%$ by comparing elastic events with charge 2 to those of charge 1. Assuming an isotropic decay distribution in the center of mass of the diffractive state, the calculated average acceptance of the counters is 95%, which agrees well with that estimated from the number of unphysical even charged multiplicity events caused either by an extra beam track or by a track missing the counters.

The corrected data are given in Tables I and II and presented in Figures 3, 4 and 5. The following features are noted:

(i) Within the statistical accuracy, the multiplicities of all three hadrons are the same when compared at the same mass available for the production of pions, $M = M_x - M_h$. This would not be true if the comparison were made at the same M_x.

(ii) The average multiplicity increases with M, approximately as $\langle n \rangle \cong 2M^{\frac{1}{2}}$, where M is in GeV, while the ratio $\langle n \rangle / D$, where $D = (\langle n^2 \rangle - \langle n \rangle^2)^{\frac{1}{2}}$, remains constant at the value of ~ 2.2 (see Fig. 3). The function $\langle n \rangle = a + b \ln (M)$ would also provide a good fit to our data but we prefer the power dependence because it characterizes the average multiplicity of many processes at higher available energy whereas a simple logarithmic dependence falls too low[2,4].

(iii) The ratio of the topological cross section σ_n to the total diffractive cross section σ (see Fig. 4) is described well by the Gaussian function

$$\frac{\sigma_n}{\sigma} = P_n = \frac{2}{\sqrt{2\pi}\, D} \, e^{-\frac{(n-n_o)^2}{2D^2}} \tag{3a}$$

where

$$n_o = 2M^{\frac{1}{2}} \text{ (M in GeV)} \tag{3b}$$

and

$$n_o/D = 2 \tag{3c}$$

The normalization of P_n is such that at any value of M the sum of P_n over odd values of n is unity to within $\sim 1\%$. In calculating values of $\langle n \rangle$ and D to compare with experimental data, one must sum over positive values of n only. This shifts the average by $\sim 4\%$ above the value of n_o and the width down by $\sim 6\%$ so that the average multiplicity becomes $\langle n \rangle = 2.08\, M^{\frac{1}{2}}$ and the $\langle n \rangle / D$ ratio is increased by 10% above the value of n_o/D, to the measured value of 2.2.

The form (3) of the probability function suggests that the multiplicity distributions satisfy KNO scaling[5]; i.e., that the product $P_n \cdot \langle n \rangle$ is a function of $n/\langle n \rangle$ only and not a function of M. Indeed, from (3a,b,c) it follows that

$$P_n \cdot n_o = 1.6 \quad e^{-2(1-n/n_o)^2} \tag{4}$$

Figure 5 shows $P_n \cdot \langle n \rangle$ versus $n/\langle n \rangle$ for the $\pi^- p$ and the pp data. Ignoring the small difference between $\langle n \rangle$ and n_o, one sees that function (4) represents the data well. In contrast to the fully inclusive reactions[6] $pp \rightarrow$ anything and $\pi p \rightarrow$ anything whose KNO scaling curve, also shown in Fig. 5, is asymmetric and peaks at $n/\langle n \rangle \cong 0.8$, the distribution for the diffractive data is symmetric about the peak at $n/\langle n \rangle = 1$.

Our results for $\langle n \rangle$ and $\langle n \rangle/D$ agree well with previous measurements[7]. However, the multiplicity distributions obtained in these measurements[7,8] are inconsistent with ours in that they follow an asymmetric scaling curve similar to that of the inclusive case. We attribute the inconsistency to their use of large M_x^2 bins needed for adequate statistics in presenting the distributions, for example $0 < M_x^2 < 32\ (\mathrm{GeV/c})^2$, which integrates the data over large variations in average and width and distorts the distributions.

In conclusion, we find that the charged multiplicity distributions of high mass diffractive pion, kaon and nucleon states follow a universal Gaussian function that depends only on the available mass M (GeV), has a peak that varies with M as $n_o \cong 2\ M^{\frac{1}{2}}$, and a peak to width ratio $n_o/D \cong 2$.

We wish to thank Gregory Snow for his participation in the running of this experiment. We are indebted to Guenter Prokesch, Donald Humbert and Ruth Snyder for their technical assistance.

REFERENCES

(a) Present address: Fermi National Accelerator Laboratory, Batavia, Illinois 60510

1. R.L. Cool et al., Phys. Rev. Lett. 47, 701 (1981).

2. K. Goulianos, H. Sticker and S. White. *Universality of Charged Multiplicity Distributions* (to be published)

3. R.L. Cool et al., Phys. Rev. D24, 2821 (1981).

4. E. Albini et al., Nuovo Cimento 32, 101 (1976) and references therein.

5. Z. Koba, H.B. Nielson and P. Olesen, Nucl. Phys. B40, 317 (1972).

6. P. Slattery, Phys. Rev. D7, 2073 (1973). For a compilation of the data, see Ref. 4 and E. DeWolf et al., Nucl. Phys. B87, 325 (1975).

7. πp : F.C. Winkelmann et al., Phys. Rev. Lett. 32, 121 (1974).

   pp : F.T. Dao et al., Phys. Lett. 45B, 399 (1973); S.J. Barish et al., Phys. Rev. Lett. 31, 1080 (1973); J.W. Chapman et al., Phys. Rev. Lett. 32, 257 (1974); and M.G. Albrow et al., Nucl. Phys. B102, 275 (1976).

   $\bar{p}p$: F. Grard et al., Phys. Lett. 59B, 409 (1975); C.P. Ward et al., Nucl. Phys. B153, 299 (1979).

8. S. Barshay et al., Phys. Rev. Lett. 32, 1390 (1974).

Figure Captions -

1. Apparatus (plan view, to scale).

2. Multiplicity counter pulse height distribution for $\pi^- p \to Xp$ at 100 GeV/c and $3 < M_x^2 < 5$ GeV^2. For each event the smaller of the two pulse heights was used.

3. The average charged multiplicity and the ratio of the average to the width as a function of available mass. The curves represent $\langle n \rangle = 2.08\ M^{\frac{1}{2}}$ and $\langle n \rangle / D = 2.2$ as discussed in the text.

4. Topological cross sections σ_n/σ versus available mass for $hp \to Xp$ ($h = \pi^-, p$).

5. The product $(\sigma_n/\sigma) \cdot \langle n \rangle$ versus $n/\langle n \rangle$ for the data presented in Figure 4. The solid line represents the Gaussian function discussed in the text (Eq. 4). The broken line is from a fit to the inclusive data $hp \to$ anything (Ref. 6).

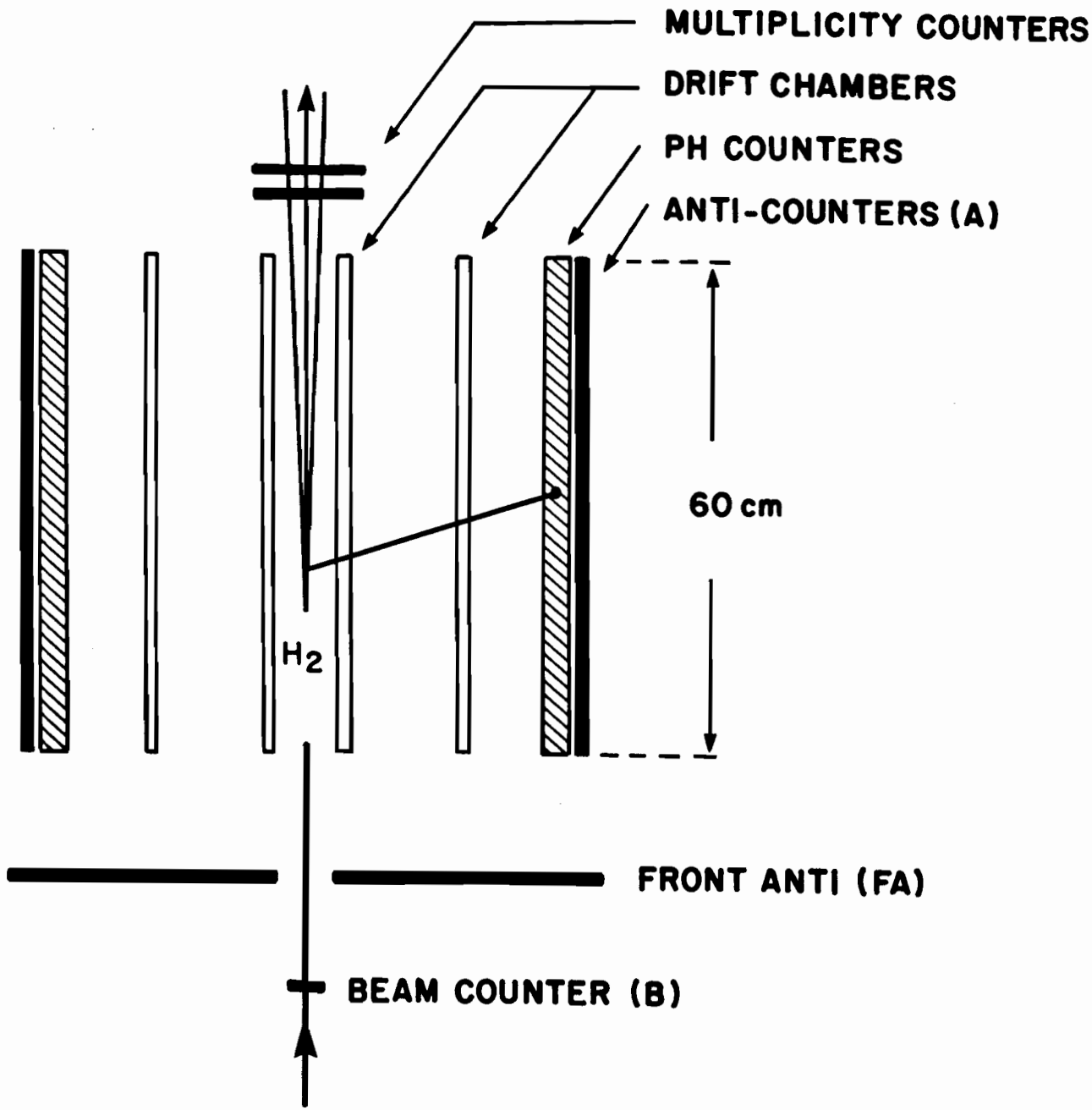
MULTIPLICITY COUNTERS
DRIFT CHAMBERS
PH COUNTERS
ANTI-COUNTERS (A)
60 cm
H_2
FRONT ANTI (FA)
BEAM COUNTER (B)

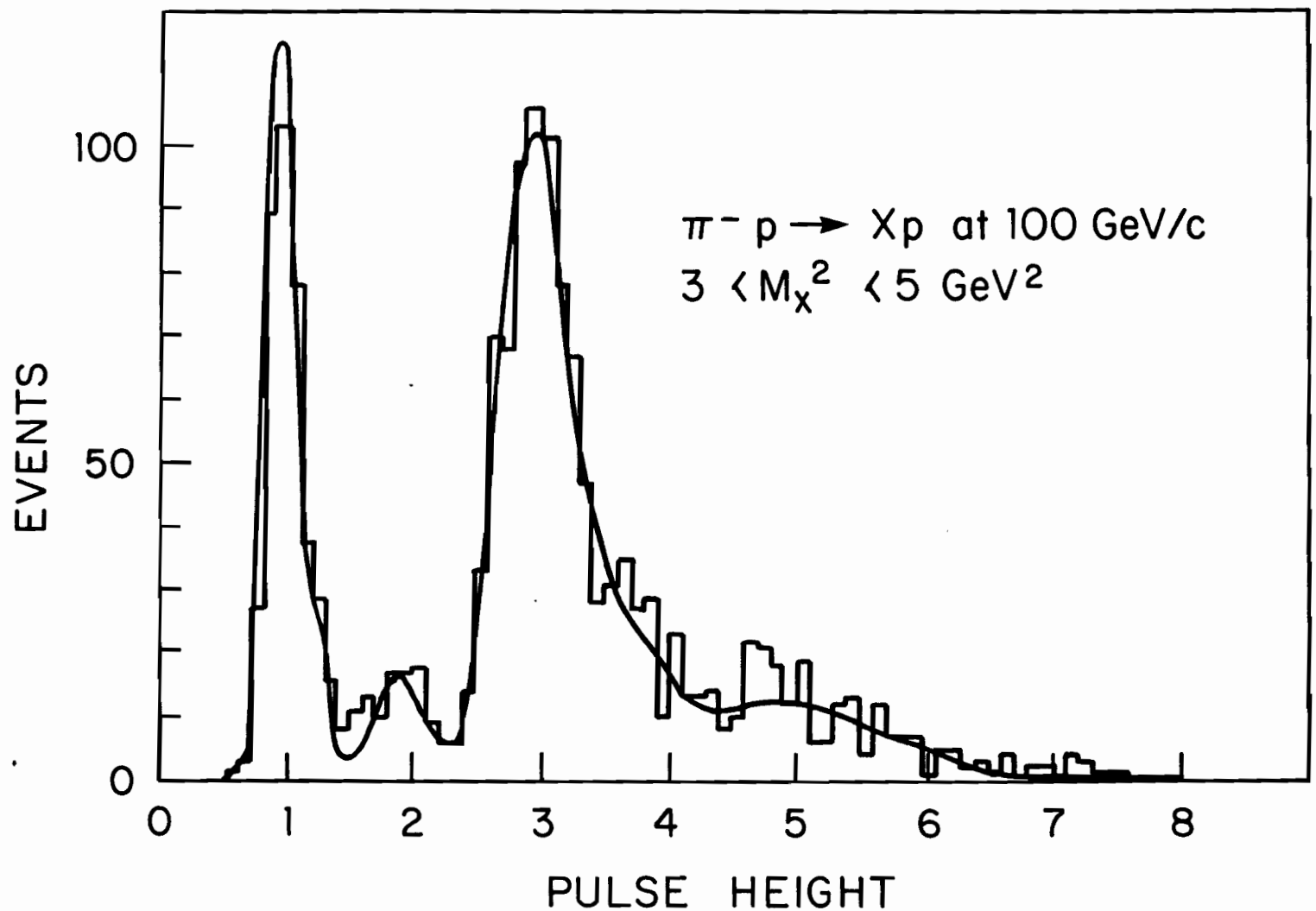
$\pi^- p \rightarrow Xp$ at 100 GeV/c
$3 < M_X^2 < 5$ GeV^2
EVENTS
100
50
0
0
1
2
3
4
5
6
7
8
PULSE HEIGHT

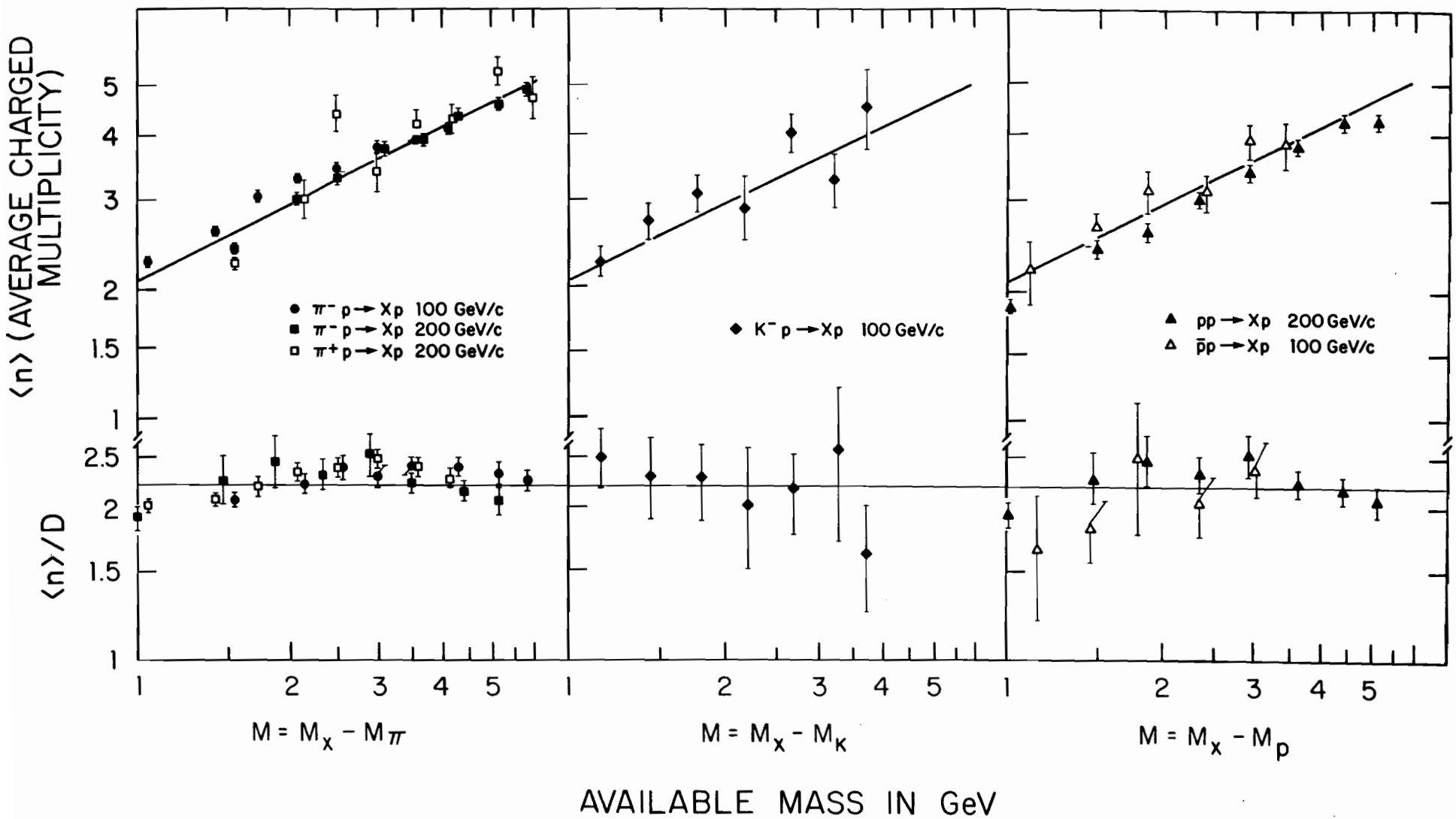
⟨n⟩ (AVERAGE CHARGED MULTIPLICITY)
⟨n⟩/D
● π⁻ p → Xp 100 GeV/c
■ π⁻ p → Xp 200 GeV/c
□ π⁺ p → Xp 200 GeV/c
◆ K⁻ p → Xp 100 GeV/c
▲ pp → Xp 200 GeV/c
△ p̄p → Xp 100 GeV/c
M = Mx − Mπ
M = Mx − MK
M = Mx − Mp
AVAILABLE MASS IN GeV

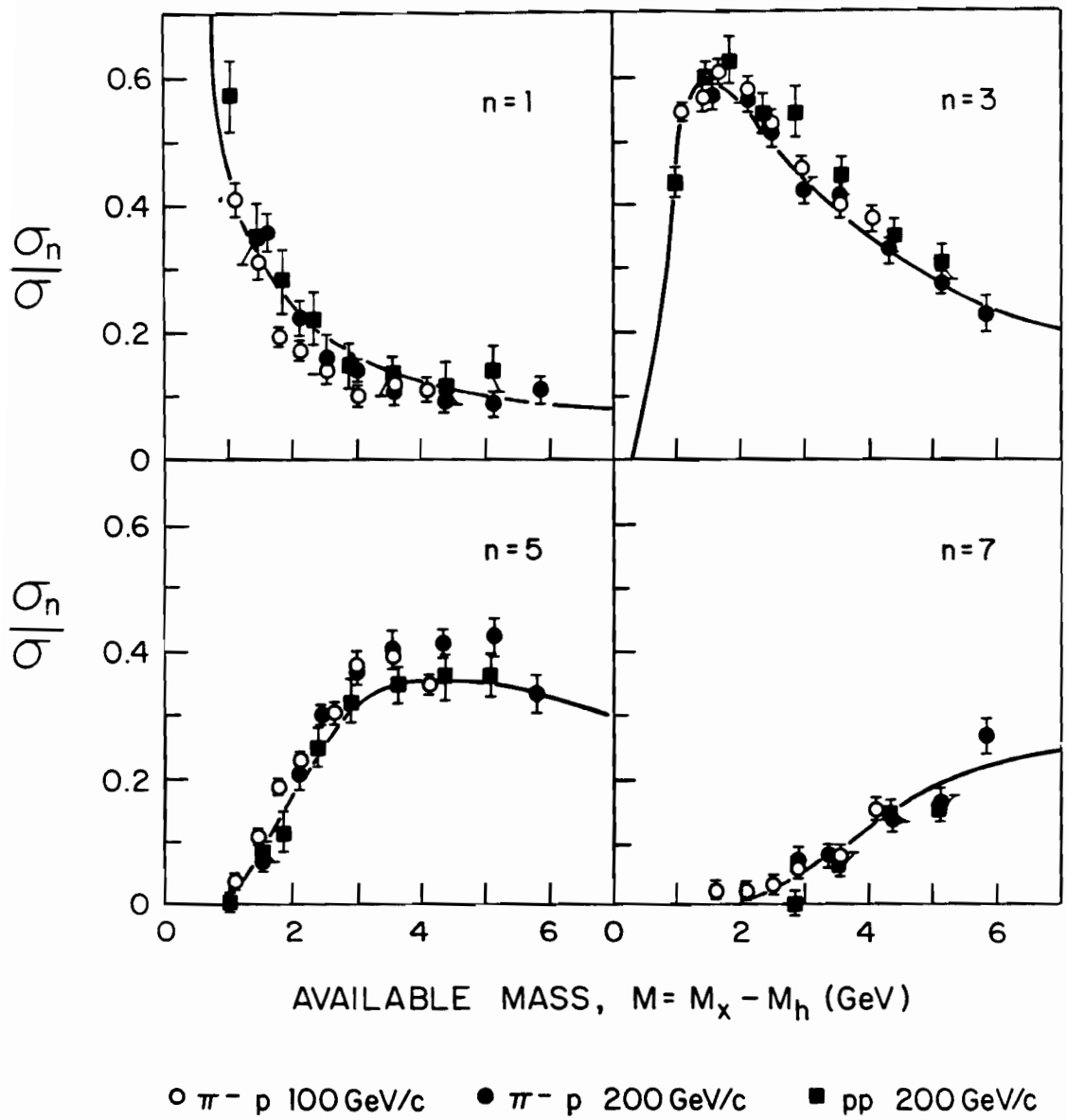
n = 1
n = 3
n = 5
n = 7
σ_n / σ
0.6
0.4
0.2
0
0
2
4
6
AVAILABLE MASS, $M = M_x - M_h$ (GeV)
○ π^- p 100 GeV/c
● π^- p 200 GeV/c
■ pp 200 GeV/c

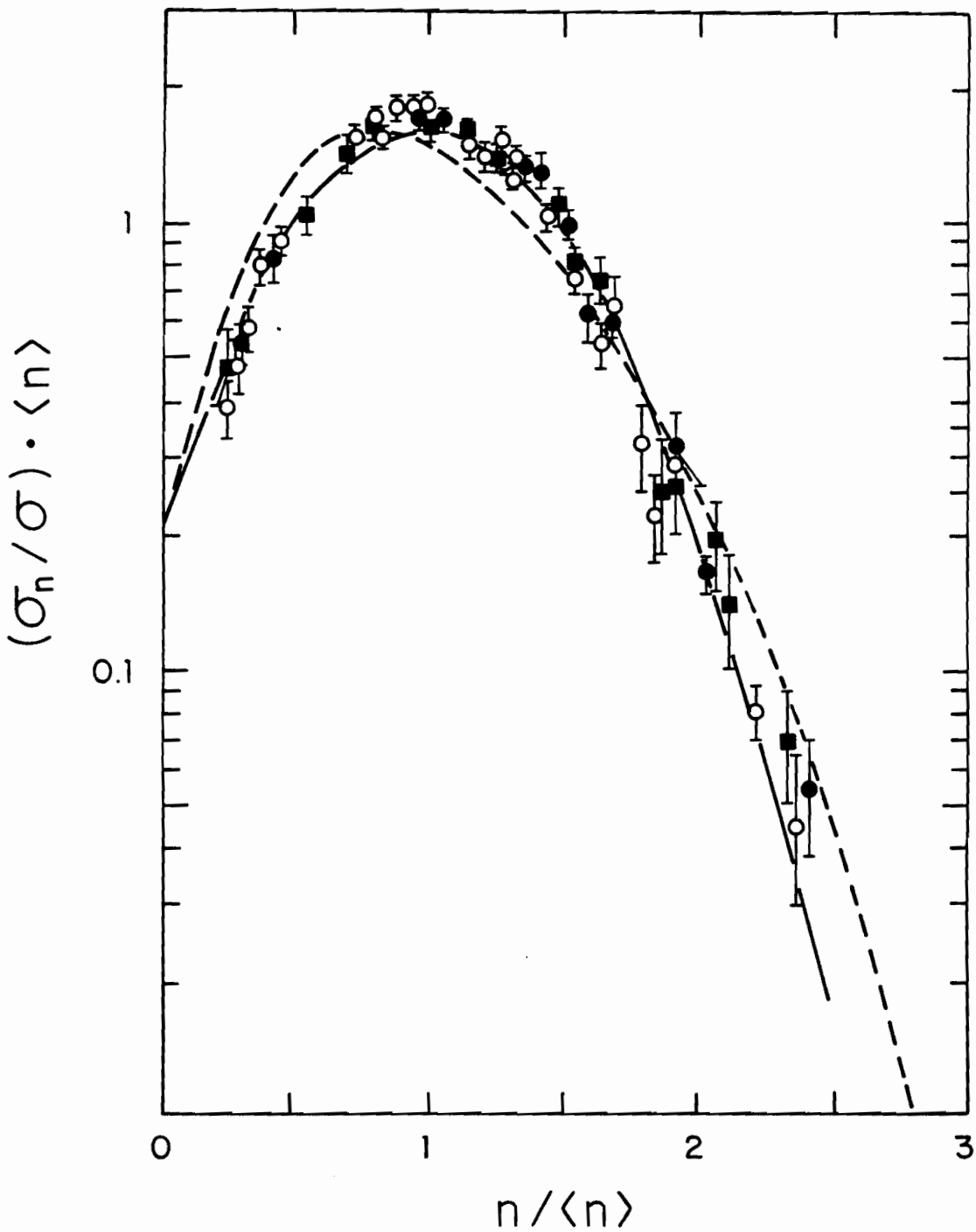
1
0.1
$(\sigma_n/\sigma)\cdot\langle n\rangle$
0
1
2
3
$n/\langle n\rangle$

TABLE I

Charged Multiplicities of X from hp → Xp at 100 GeV/c

h	M $(M_x - M_h)$	$\bar{n}$	D $(\overline{n^2} - \bar{n}^2)^{\frac{1}{2}}$	$\bar{n}/D$	σ_n/σ n=1	n=3	n=5	n=7
π^-	1.06	2.25±0.04	1.12±0.02	2.02±0.05	0.41±0.03	0.55±0.01	0.04±0.01	
	1.43	2.60±0.05	1.25±0.03	2.08±0.06	0.31±0.03	0.57±0.02	0.11±0.01	
	1.73	3.05±0.07	1.33±0.06	2.30±0.11	0.19±0.02	0.61±0.02	0.18±0.02	0.02±0.01
	2.08	3.20±0.06	1.36±0.05	2.35±0.11	0.17±0.02	0.58±0.02	0.23±0.01	0.02±0.01
	2.50	3.44±0.07	1.43±0.06	2,41±0.11	0.14±0.02	0.53±0.02	0.30±0.02	0.03±0.01
	2.99	3.79±0.07	1.51±0.05	2.51±0.09	0.10±0.02	0.46±0.02	0.38±0.02	0.06±0.01
	3.59	3.91±0.09	1.64±0.06	2.39±0.10	0.12±0.02	0.40±0.02	0.39±0.02	0.08±0.02
	4.09	4.14±0.09	1.82±0.05	2.28±0.08	0.11±0.02	0.38±0.02	0.34±0.02	0.16±0.02
K^-	0.79	2.08±0.12	1.03±0.06	2.03±0.17	0.47±0.08	0.52±0.06	0.01±0.02	
	1.15	2.26±0.14	0.91±0.11	2.50±0.35	0.35±0.09	0.66±0.09	-0.01±0.02	
	1.43	2.69±0.24	1.17±0.19	2.30±0.42	0.26±0.09	0.63±0.10	0.10±0.07	
	1.77	3.05±0.24	1.35±0.20	2.25±0.37	0.20±0.07	0.59±0.09	0.19±0.07	0.02±0.03
	2.18	2.87±0.39	1.42±0.37	2.02±0.59	0.28±0.12	0.50±0.13	0.21±0.09	0.00±0.07
	2.67	3.48±0.36	1.62±0.26	2.14±0.41	0.17±0.07	0.49±0.10	0.28±0.09	0.06±0.08
	3.26	3.23±0.38	1.26±0.42	2.57±0.90	0.16±0.08	0.55±0.11	0.31±0.10	-0.02±0.08
	3.76	4.52±0.83	2.80±0.38	1.61±0.37	0.30±0.14	0.23±0.22	-0.09±0.21	0.55±0.23
$\bar{p}$	0.58	1.85±0.15	1.12±0.13	1.65±0.23	0.61±0.11	0.34±0.06	0.05±0.03	
	0.89	1.93±0.19	1.10±0.17	1.76±0.32	0.56±0.13	0.41±0.09	0.03±0.03	
	1.15	2.18±0.30	1.32±0.33	1.65±0.47	0.47±0.14	0.52±0.12	-0.02±0.05	0.04±0.04
	1.47	2.65±0.18	1.47±0.19	1.80±0.26	0.33±0.05	0.56±0.17	0.06±0.04	0.05±0.03
	1.86	3.13±0.32	1.26±0.34	2.49±0.73	0.09±0.08	0.82±0.12	0.01±0.07	0.07±0.06
	2.33	3.12±0.25	1.54±0.18	2.03±0.28	0.25±0.08	0.46±0.09	0.27±0.07	0.02±0.04
	2.90	3.92±0.29	1.64±0.18	2.39±0.31	0.07±0.05	0.52±0.11	0.27±0.09	0.13±0.06
	3.39	3.86±0.41	1.08±0.46	3.57±1.55	0.05±0.08	0.43±0.11	0.55±0.12	-0.04±0.09

TABLE II

Charged Multiplicities of X from hp → Xp at 200 GeV/c

h	M $(M_x - M_h)$	$\bar{n}$	D $(\overline{n^2} - \bar{n}^2)^{\frac{1}{2}}$	n/D	σ_n/σ n=1	n=3	n=5	n=7
π^-	1.55	2.40±0.05	1.15±0.03	2.09±0.07	0.36±0.03	0.57±0.01	0.07±0.01	
	2.08	3.00±0.08	1.35±0.06	2.22±0.11	0.22±0.03	0.57±0.02	0.20±0.02	
	2.50	3.29±0.09	1.36±0.07	2.41±0.14	0.17±0.03	0.53±0.03	0.30±0.02	
	2.99	3.73±0.09	1.63±0.05	2.30±0.09	0.14±0.02	0.42±0.02	0.37±0.02	0.07±0.02
	3.59	3.91±0.09	1.62±0.06	2.41±0.11	0.11±0.02	0.41±0.02	0.40±0.03	0.08±0.02
	4.29	4.38±0.09	1.83±0.06	2.40±0.10	0.09±0.02	0.33±0.02	0.41±0.02	0.14±0.02
	5.13	4.60±0.13	1.97±0.09	2.33±0.12	0.09±0.02	0.28±0.02	0.42±0.03	0.16±0.03
	5.84	4.90±0.15	2.18±0.08	2.25±0.11	0.11±0.02	0.23±0.03	0.33±0.03	0.27±0.03
π^+	1.55	2.24±0.12	1.10±0.06	2.04±0.16	0.41±0.08	0.55±0.06	0.03±0.02	
	2.08	3.00±0.25	1.46±0.18	2.05±0.30	0.24±0.07	0.56±0.09	0.17±0.08	0.03±0.03
	2.50	4.43±0.37	1.97±0.18	2.25±0.28	0.08±0.07	0.44±0.10	0.18±0.09	0.31±0.09
	2.99	3.39±0.29	1.46±0.25	2.32±0.45	0.16±0.06	0.52±0.08	0.29±0.07	0.03±0.06
	3.59	4.21±0.28	1.59±0.18	2.64±0.35	0.07±0.05	0.37±0.08	0.44±0.09	0.11±0.07
	4.29	4.31±0.28	1.90±0.15	2.26±0.23	0.10±0.05	0.37±0.07	0.34±0.08	0.16±0.07
	5.13	5.31±0.34	1.91±0.23	2.78±0.38	0.00±0.05	0.33±0.08	0.21±0.08	0.41±0.09
	5.84	4.73±0.45	2.18±0.22	2.17±0.30	0.13±0.08	0.19±0.10	0.41±0.11	0.19±0.12
p	0.99	1.87±0.06	0.97±0.05	1.92±0.11	0.57±0.06	0.43±0.02	0.00±0.01	
	1.47	2.40±0.10	1.05±0.12	2.28±0.28	0.35±0.05	0.59±0.03	0.08±0.02	-0.02±0.01
	1.86	2.60±0.11	1.05±0.12	2.47±0.31	0.28±0.05	0.62±0.04	0.12±0.03	-0.02±0.01
	2.33	3.01±0.11	1.29±0.09	2.33±0.18	0.22±0.04	0.54±0.03	0.25±0.03	-0.02±0.01
	2.90	3.39±0.13	1.33±0.12	2.54±0.24	0.14±0.04	0.54±0.04	0.32±0.04	0.00±0.02
	3.59	3.82±0.12	1.72±0.08	2.22±0.12	0.13±0.03	0.44±0.03	0.35±0.03	0.07±0.02
	4.41	4.24±0.15	1.96±0.08	2.16±0.12	0.12±0.03	0.35±0.03	0.36±0.04	0.14±0.03
	5.12	4.26±0.17	2.06±0.09	2.07±0.13	0.14±0.04	0.31±0.03	0.36±0.04	0.15±0.03